

# Microhardness properties of Cu–W amorphous thin films

N. RADIĆ

*Department of Materials Science, Ruđer Bošković Institute, Bijenička 54,  
POB 1016, 10001 Zagreb, Croatia  
E-mail: radic@rudjer.irb.hr*

M. STUBIČAR

*Department of Physics, Faculty of Sciences, University of Zagreb, Bijenička 32, POB 162,  
10001 Zagreb, Croatia*

Pure copper, pure tungsten and amorphous  $\text{Cu}_{50}\text{W}_{50}$  and  $\text{Cu}_{66}\text{W}_{34}$  alloy films were deposited by the direct current magnetron sputtering technique on cooled glass substrates. The film microhardness has been investigated as a function of alloy composition and substrate potential bias during deposition. The microhardness exhibited a maximum at Cu concentrations close to 50 at%, similar to the case of completely miscible binary alloys. The ion bombardment caused by the negative substrate polarization increased the film microhardness. The annealing of the amorphous Cu–W films up to 250 °C in vacuum increased the film microhardness by 10–20% apparently owing to the formation of the W(Cu) crystalline phase dispersed within a predominantly amorphous film matrix. © 1998 Kluwer Academic Publishers

## 1. Introduction

The development of alloys of immiscible binary systems is largely constrained by inherent limitations of a conventional equilibrium (metallurgical) processing, which in such cases results in gross chemical segregation. Within these systems, refractory transition-metal alloys are of particular interest because of their possible application in microelectronics and thin-film coatings. Tungsten-based alloys are promising in that respect [1–4], and there were many attempts by various methods to produce the Cu–W alloys. As expected, owing to the non-equilibrium processing, the ranges of chemical and phase compositions of the alloys prepared by vapour quenching [1, 5], codeposition sputtering [1, 6, 7], mechanical alloying [8, 9] and ion-beam mixing or irradiation [10, 11] differ widely. Thus, the samples with a microcrystalline [5], a microcrystalline + amorphous mixture [1, 9] and a completely amorphous [2, 7] structure were obtained. Their structural [1, 2, 5, 7, 9], mechanical [5], electrical [5] and electronic [2, 12] properties were examined, as well as their thermal stability and crystallization temperature of amorphous samples of various compositions [1, 7, 13, 14].

In this work the investigation of the microhardness properties of amorphous Cu–W thin films, prepared by the sputtering technique, is presented. The effects of the sample compositions and preparation conditions upon the micromechanical properties were examined. Selected amorphous samples were isothermally annealed and the dependence of the microhardness on temperature was determined. The complementary

results on the thermal stability and electrical properties of congruent amorphous Cu–W samples have been presented elsewhere [7, 12–14].

## 2. Experimental procedures

### 2.1. Sample preparation

The thin metal films were prepared on glass substrates in a sputtering apparatus described in more detail elsewhere [7]. Two independently controlled sputtering sources (with pure Cu and pure W targets) were of the cylindrical magnetron configuration. Argon at a pressure of 5 Pa in a constant flow mode served as the working gas. The discharge parameters varied within the following limits: a cathode current density of 4–7 mA cm<sup>-2</sup> for W, and 5–15 mA cm<sup>-2</sup> for Cu; the corresponding voltages were in the ranges 450–550 V for W, and 350–450 V for Cu. Thus, the composition of the prepared films varied within a fairly wide range.

With rather constant deposition parameters (working gas pressure, discharge current and voltage, substrate temperature and deposition time) during the preparation of one series of samples, the principal variable parameter was the substrate holder potential bias with respect to the discharge plasma. Generally, three polarizations were applied: firstly a voltage bias,  $U_p$  of –50 V, with respect to the discharge plasma (grounded anode) and the total ion current drawn from the adjacent plasma in the range of a few milliamperes; secondly, the substrate at a floating potential of about –5 V with respect to the plasma, and zero net current to the substrate holder; thirdly a positive

holder polarization of about a few volts with respect to the plasma and a total electron current extracted from the plasma to the substrate holder fixed at  $I_p = 50$  mA.

## 2.2. Sample characterization

Pure copper and tungsten films, as well as the amorphous  $\text{Cu}_{50}\text{W}_{50}$  and  $\text{Cu}_{66}\text{W}_{34}$  alloy films were prepared. The composition of alloy films was estimated from the film growth rates measured for both pure W and pure Cu, as well as from the ratio of discharge currents during deposition. In our previous work [7], the sample compositions were estimated in the same way and checked by an X-ray fluorescence method. The agreement was fairly good (within 10% relative error). Sample compositions given in this work are nominal in that sense. The thickness of the films was measured by an Alpha Step surface profilometer.

The film structure and phase composition were determined by an X-ray diffraction (XRD) method using a Philips PW 1820 vertical goniometer with monochromatized  $\text{Cu K}\alpha$  radiation.

The microhardness (hardness microindentation measurement) was measured by means of an E. Leitz Miniload II apparatus under a 0.0981 N load, with a loading time of 10 s. The indentation patterns produced during the microhardness measurements were observed using an optical Metallux 3 type microscope. Ten indentations were performed to obtain an average microhardness value.

Completely amorphous samples were isothermally annealed in vacuum better than  $10^{-3}$  Pa at 100, 150, 200 and 250 °C consecutively, for 30 min. After annealing, the microhardness was measured at room temperature. The microhardness properties can be interpreted on the basis of XRD measurements performed in this work, as well as in our previous work [7]. Post-annealing XRD examination was also undertaken.

## 3. Results

### 3.1. Structure of the as-deposited films

The actual deposition conditions ( $p_{\text{Ar}} = 5$  Pa and  $T_s = 180\text{--}200$  K) result in the expected structure of pure metal films deep in zone 1 of the Thornton [15] microstructure zone diagram. A columnar porous structure, with small grains separated by a number of voids of considerable size, has been found in tungsten films formed by sputter deposition under conditions similar to those employed in our experiments [16, 17]. Such microstructure is essentially stress free owing to small intercolumnar coupling [17]. In copper films deposited under the same conditions, a similar microstructure might be expected. XRD examination of the as-prepared thin films of pure copper and pure tungsten showed that the intensities of some diffraction lines were much stronger than expected according to the standard diffraction patterns: the 1 1 1 line for Cu, and the 1 1 0 for W. This indicated the presence of the preferred orientation of the crystal grains in these

films, with the (1 1 1) plane parallel to the film surface for Cu and the (1 1 0) plane parallel to the thin film surface for W. From the half-width of the highest peak in the XRD pattern of the tungsten film (Fig. 1), the average linear dimension of the grains in this film was estimated to be  $L_W \approx 30\text{--}45$  Å (according to Scherrer's formula). These results were at the lower end of the respective grain size ranges estimated by Dirks and van den Broek [5]. Larger grain sizes were observed by other researchers: 50–100 Å grains in very thin tungsten films [16], 125 Å grains in films 1000 Å thick [11], and grains of 200–400 Å diameter in submicron tungsten films [17]. All these studies

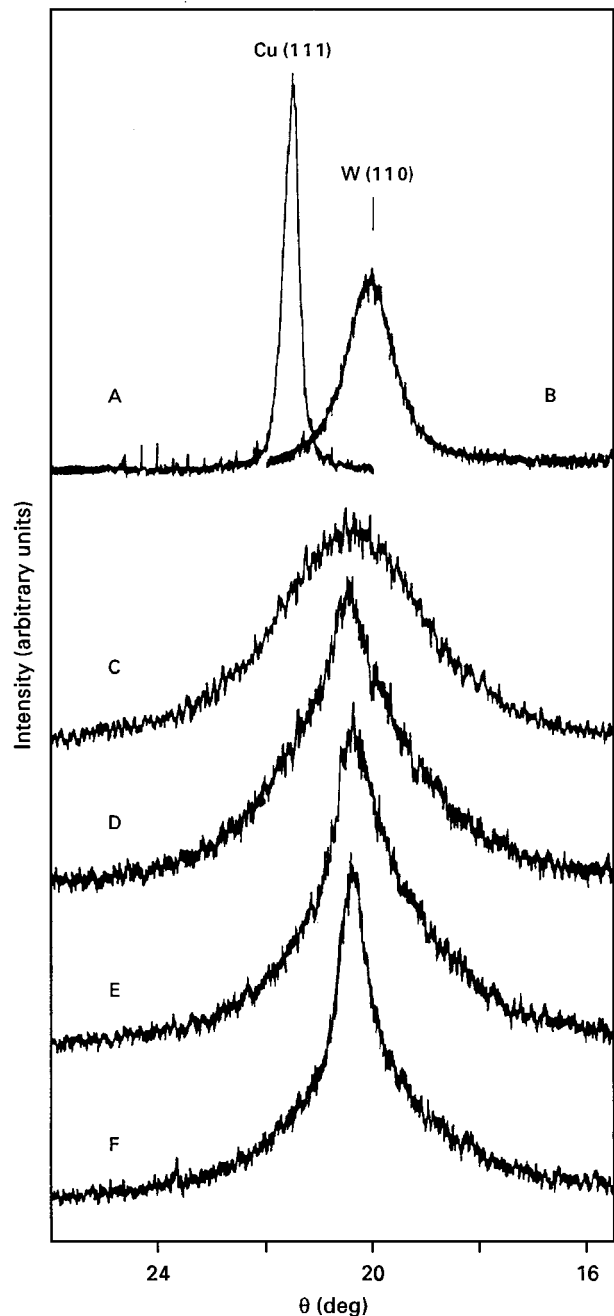


Figure 1 XRD patterns of the as-prepared thin-film samples: Curve A, pure copper; Curve B, pure tungsten; Curves C–F, Cu–W thin films containing approximately 50 at% Cu, from completely amorphous alloy (Curve C), to predominantly crystalline (Curve F). Diffraction intensities for both pure copper and pure tungsten are reduced twice with respect to those of curves C–F.

agreed that the observed small grains consist of a metastable  $\beta$ -W phase, while the stable  $\alpha$ -W phase body centered cubic (b.c.c) exhibits larger grains (1000–3000 Å) and it is generally related to the T zone in the Thornton microstructure diagram. It is noteworthy that we have obtained small-grained films consisting of the stable  $\alpha$ -W phase, which have otherwise required special cleanliness precautions [17]. It seemed that, as the film deposition front departed from the cooled substrate, its surface temperature exceeded the  $\beta$ -W  $\rightarrow$   $\alpha$ -W transition temperature (approximately 135 °C [16]), while still being low enough to prevent grain-boundary migrations. As a result, a small-grained  $\alpha$ -W phase was formed. However, in tungsten films of 0.5  $\mu\text{m}$  (or less) thickness, the  $\beta$ -W phase appeared and also in still thinner films, as observed by Petroff *et al.* [16]. There was no noticeable effect of the substrate polarization (within the bias range investigated in this work) to the size of grains and their orientation as observed by the XRD method.

The Cu–W alloys were prepared in the nominal compositions of 50 at% Cu and 66 at% Cu. Apart from completely amorphous samples, the samples with a mixture of amorphous and crystalline phases or predominantly a crystalline phase have been occasionally obtained, as well. The crystalline phase was tentatively identified as a metastable W(Cu) solid solution with the b.c.c. lattice [5,9,13]. A selection of characteristic shapes of the strongest XRD signals obtained for various samples containing 50 at% Cu is presented in Fig. 1.

### 3.2. Microhardness measurements

The samples characterized by the XRD method were examined by the microhardness measurements. Only the completely amorphous Cu–W films were considered for comparison with both the pure copper and the pure tungsten films deposited under the same conditions. The results are presented in Fig. 2. The error bars which amounted to approximately  $\pm 5\%$  were omitted for clarity. Some comments are now made about the above results.

(a) It is well known that the correct value of the thin film microhardness strongly depends upon the appropriate load used in the indentation process mainly because of the anvil effect. Several models which allowed the interpretation of hardness tests performed on layered materials were proposed [18–20]. The principal parameter governing their implementation was the ratio of the indentation depth,  $d$ , to the film thickness,  $t$ . If the  $d/t$  ratio exceeded a certain critical value, the measured hardness was no longer characteristic only for the coating but also included the contribution from the substrate hardness. The critical value of  $d/t$  ranged from 0.07 for the hard film on a soft substrate to 1.0 for the opposite case. The minimal load allowed in the employed Leitz equipment was 5 g. However, in order to improve the accuracy of the optical reading of the size of indentation traces, in all measurements a standard load of 10 g has been used. Thus, we have investigated the possible effects of the

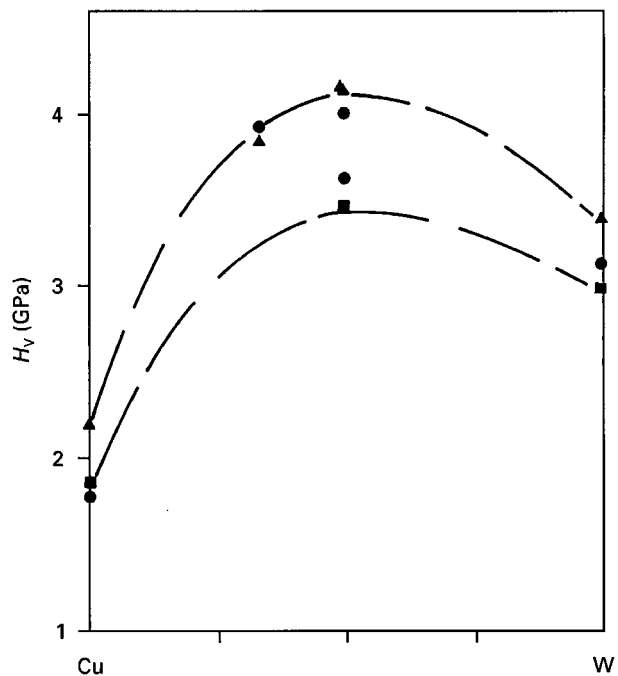


Figure 2 Vickers microhardness variation with the thin-film composition (in atomic per cent) and the substrate polarization during deposition. (■) electrically floating substrate; (●) positive potential bias; (▲) negative potential bias; (---), lines which are only guidance for the eye. The samples having 50 at% Cu and 66 at% Cu were completely amorphous.

glass substrate hardness upon the results of the microhardness measurements for metal films of the order of a micron thick. To this end, a series of six copper films with nominally halved thickness between consecutive samples was deposited on the glass substrate. The actual thickness of the two thickest films was measured with an Alpha Step apparatus, resulting in 0.9  $\mu\text{m}$ , and 0.37  $\mu\text{m}$ , respectively. The results of microhardness measurements on the series of Cu films are presented in Fig. 3. The film thickness was taken to be the nominal thickness on the abscissa axis in order to present a graph of the microhardness values for very thin films. Although the results were somewhat scattered, the anvil effect of the glass substrate was obviously quite pronounced in the submicron films. Without performing a rigorous analysis, the approximate film thickness at which the substrate contribution to the measured microhardness on film vanished could be estimated from Fig. 3. Assuming the bulk value of copper microhardness ( $0.96 \pm 0.06$  GPa, as measured on the bulk copper cathode) to be the limit of the film “bulkiness”, it appeared that the glass substrate effects vanished in the copper films approximately 1.7–2  $\mu\text{m}$  thick. As the indentation depth on bulk copper is 2  $\mu\text{m}$  in actual conditions, the above estimate agreed well with the critical value  $d/t = 1$  derived from the model of a soft film on a hard substrate in [20]. Since copper is a soft material when compared with the others examined, one can presume that the glass substrate effects are less pronounced in other (thicker) metallic films examined in this work. In that sense, the microhardness values for pure copper films appearing in Fig. 2 were probably more affected by the film thickness or substrate effects than by the

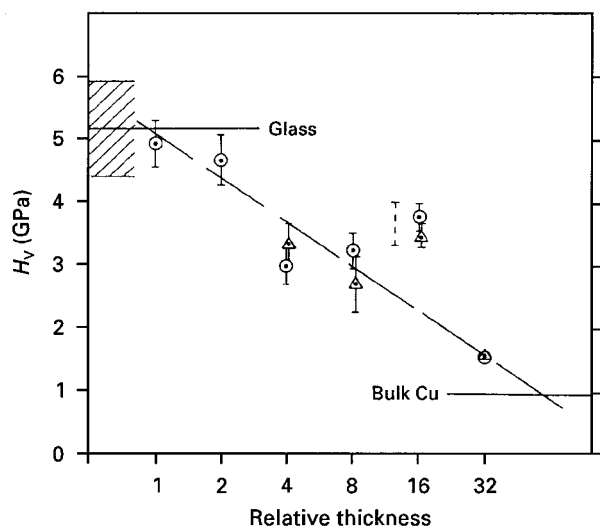


Figure 3 The effects of copper film thickness upon the measured microhardness value. ( $\Delta$ ), ( $\circ$ ), results of the two series of measurements on the same film. The broken vertical bar denotes the position of the measured thickness of the second sample ( $0.37\ \mu\text{m}$ ) relative to the measured thickness of the first sample ( $0.9\ \mu\text{m}$ )

variation in deposition conditions (substrate polarization). On the tungsten side of Fig. 2, the microhardness values of pure W films are about the half of the bulk value of  $6.66 \pm 0.23\ \text{GPa}$ , as measured on the polished W cathode (the value of the bulk microhardness for pure (99.95% or more) tungsten rods is  $6.51\ \text{GPa}$ ). A relatively low microhardness of tungsten films resulted from their porous columnar microstructure, as determined in films grown under similar conditions by other writers [15–17]. The intercolumnar voids were the cause of the low mechanical strength of the examined tungsten films, thus providing space for easy mechanical deformations.

(b) As seen in Fig. 2, amorphous  $\text{Cu}_{50}\text{W}_{50}$  and  $\text{Cu}_{66}\text{W}_{34}$  samples exhibited higher microhardness than both pure copper and pure tungsten films. Since those samples were a few micrometres thick, and the indentation depths were about  $1\ \mu\text{m}$ , it might be safely assumed that the glass substrate effects (if any) are negligible [20, 21]. The qualitative dependence of the microhardness upon the composition resembled the curves obtained for the completely miscible transition-metal binary alloys [22]. The fact that copper and tungsten are immiscible, and that their amorphous alloys crystallize at a relatively low temperature, apparently had no consequence on the overall shape of the microhardness versus composition dependence. It seems that the observed behaviour might be simply explained by the effect of alloying (solid solution hardening), i.e., the alloys usually exhibited higher hardness values than their pure components.

(c) The effects of substrate bias during deposition upon the microhardness of the measured films were small but consistent. Generally, the films deposited on the electrically floating surface were less hard than those deposited under the additional bombardment of net ion or electron flux drawn from the adjacent plasma. Generally, negatively polarized substrates yielded the samples with the highest microhardness.

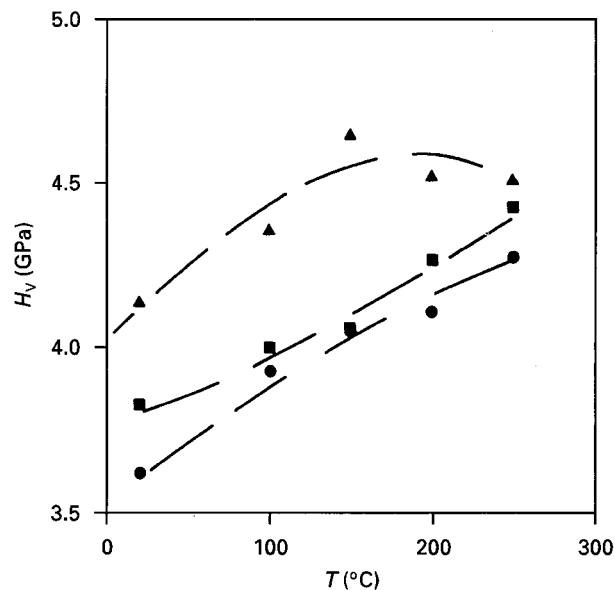


Figure 4 Microhardness variation of the completely amorphous samples with the annealing temperature. ( $\blacktriangle$ ),  $\text{Cu}_{50}\text{W}_{50}$  alloy, negative polarization; ( $\blacksquare$ ),  $\text{Cu}_{66}\text{W}_{34}$  alloy, negative polarization; ( $\bullet$ ),  $\text{Cu}_{50}\text{W}_{50}$  alloy, positive polarization; (---) lines which are only guidance for the eye.

The mechanism of this small *in-situ* hardness increase was probably due to the ion peening effect [23]. A more compact film structure with less intercolumnar voids was formed owing to ion bombardment. The small overall increase in microhardness was a consequence of the low energy of impinging ions acquired within the plasma sheath.

(d) Finally, the results of microhardness measurements on predominantly crystalline samples should be mentioned. In various visually discernible belts at the surface of the W(Cu) metastable solid solution samples (the XRD pattern in Fig. 1, curve F), the average microhardness ranged from  $4.30$  to  $5.20\ \text{GPa}$ .

### 3.3. Thermal annealing

The effects of thermal treatment in vacuum on the microhardness of the completely amorphous samples are shown in Fig. 4. The annealing temperatures have successively increased in equal steps of  $50\ ^\circ\text{C}$ . As seen, up to the highest annealing temperature ( $250\ ^\circ\text{C}$ ) the microhardness of all three samples almost monotonically increased by 10–20% above the initial values. However, the data scattering within one series of microhardness measurements has increased, as well, thus resulting in an increase in the standard deviation (5%) for the as-prepared samples to approximately 10% after the heat treatment of samples at  $250\ ^\circ\text{C}$ . This indicated that some sort of segregation process occurred during the annealing which destroyed lateral homogeneity of the film. As found in earlier studies on the thermal stability of similar Cu–W films [7, 13, 14], within the examined temperature range only a pure copper precipitation, starting at about  $150\ ^\circ\text{C}$ , can be detected by the XRD method. However, the monotonic increase in the microhardness from room temperature to  $250\ ^\circ\text{C}$  indicated that the process of the Cu

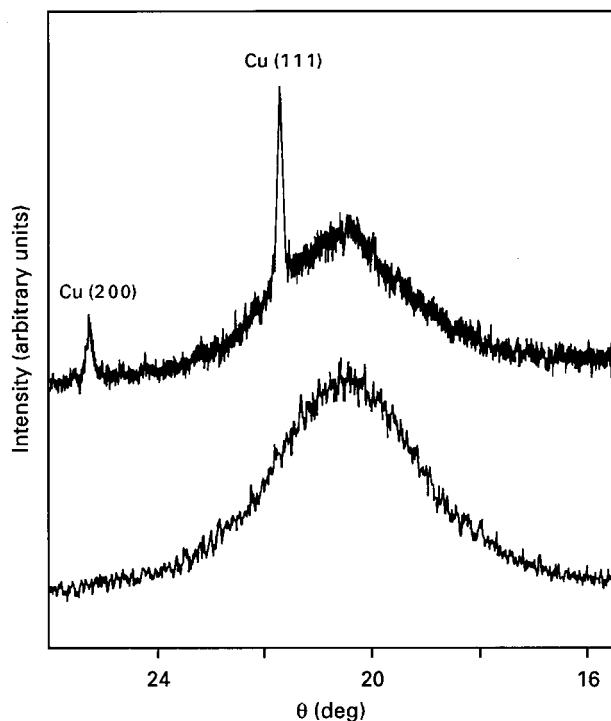


Figure 5 Pre- and post-annealing XRD patterns of the initially completely amorphous sample  $\text{Cu}_{50}\text{W}_{50}$  (lower curve and upper curve, respectively). The intensity scales are the same for both signals. At 250 °C, only pure copper segregation is clearly detectable by the XRD method.

segregation in Cu–W amorphous films probably took place at even lower temperatures, with the presumed formation of the W(Cu) solid solution in the residual amorphous matrix in quantities below the detection limits of the XRD method. The XRD patterns of annealed samples exhibit only a prominent Cu signal superimposed upon the still prevailing pattern of the amorphous Cu–W matrix (Fig. 5). Thus, the observed hardening of the amorphous Cu–W films caused by the annealing might be tentatively explained as due to their partial crystallization, which introduced a mixture of two phases leading to the increase in hardness and strength of material (dispersion hardening effect). Since pure copper is less hard than the amorphous Cu–W matrix, it is suggested that the nucleation-and-growth process of W(Cu) phase might have been taken place and it remained undetected by the XRD method.

## Conclusions

1. A series of thin film alloys of the immiscible binary Cu–W system has been prepared by the cosputtering technique in a tandem magnetron device. It has been found that most of the as-deposited samples are amorphous with the occasional appearance of the W(Cu) solid solution crystalline phase.

2. The microhardness of the prepared samples exhibits a broad maximum amounting to approximately 4.0 GPa at approximately  $\text{Cu}_{50}\text{W}_{50}$  composition, with the overall dependence upon composition similar to the case of completely miscible binary systems.

3. The film microhardness is enhanced by about 10% if during deposition the substrate is biased at – 50 V. It is probably due to the more compact film structure produced by the ion peening effect.

4. It has been shown that annealing in vacuum up to 250 °C increases the film microhardness by 10–20%. It is suggested that the observed hardening is due to the nucleation and growth of the crystalline W(Cu) phase which contributes to the sample hardness.

## Acknowledgements

The authors thank A. Pavlešin for technical assistance with the sample preparation and T. Žic for recording the XRD patterns.

## References

1. M. NASTASI, F. W. SARIS, L. S. HUNG and J. W. MAYER, *J. Appl. Phys.* **58** (1985) 3052.
2. M. A. ENGELHARDT, S. S. JASWAL and D. SELLMYER, *Phys. Rev. B* **44** (1991) 12671.
3. K. HASHIMOTO *et al.*, *Mater. Sci. Engng.* **A133** (1991) 22.
4. H. LANGE, W. MOHLING and G. MARXSEN, *Thin Solid Films* **205** (1991) 47.
5. A. G. DIRKS and J. J. VAN DER BROEK, *J. Vac. Sci. Technol.* **A3** (1985) 2618.
6. K. D. AYLESWORTH, S. S. JASWAL, M. A. ENGELHARDT, Z. R. ZHAO and D. J. SELLMYER, *Phys. Rev. B* **37** (1988) 2426.
7. N. RADIĆ, B. GRŽETA, D. GRACIN and T. CAR, *Thin Solid Films* **228** (1993) 225.
8. A. N. PATEL and S. DIAMOND, *Mater. Sci. Engng* **98** (1988) 329.
9. E. GAFFET, C. LOUISON, M. HERMELIN and F. FAUDOT, *ibid.* **A134** (1991) 1380.
10. Z. L. WANG, J. F. M. WESTENDROP and F. W. SARIS, *Nucl. Instrum. Methods*, **209–210** (1983) 115.
11. G. GLADYSZEWSKI, PH. GOUDEAU, A. NAUDON, CH. JAOUEN and J. PACAUD, *Mater. Lett.* **12** (1992) 419.
12. J. IVKOV, T. CAR, N. RADIĆ and B. BABIĆ *Solid State Commun.* **88** (1993) 633.
13. B. GRŽETA, N. RADIĆ, D. GRACIN and T. DOŠLIĆ, *Mater. Sci. Forum* **133–136** (1993) 913.
14. B. GRŽETA, N. RADIĆ, D. GRACIN and T. DOŠLIĆ and T. CAR, *J. Non-Cryst. Solids* **170** (1994) 101.
15. J. A. THORNTON, *J. Vac. Sci. Technol.* **11** (1974) 666.
16. P. PETROFF, T. T. SHENG, A. K. SINHA, G. A. ROZ-GONYI and F. B. ALEXANDER, *J. Appl. Phys.* **44** (1973) 2545.
17. A. M. HAGHIRI - GOSNET, F. R. LADAN, C. MAYEAUX and H. LAUNOIS, *J. Vac. Sci. Technol.* **A7** (1989) 2663.
18. B. JÖNSSON and S. HOGMARK, *Thin Solid Films*, **114** (1984) 257.
19. P. J. BURNETT and D. S. RICKERBY, *ibid.* **148** (1987) 41.
20. D. LÉBOUVIER, P. GILORMINI and E. FELDER, *ibid.* **172** (1989) 227.
21. I. MANIKA and J. MANIKS, *ibid.* **208** (1992) 223.
22. H. O'NEILL, "Hardness measurement of metals and alloys" (Chapman & Hall, London, 2nd Edn, 1967) p. 110.
23. F. M. D'HEURLE, *Metall. Trans.* **1** (1970) 725.

Received 11 November 1996  
and accepted 3 April 1998